Appl Nanosci (2015) 5:449–456
DOI 10.1007/s13204-014-0337-y

ORIGINAL ARTICLE

Synthesis and characterization of undoped and cobalt-doped TiO_2 nanoparticles via sol–gel technique

S. Mugundan · B. Rajamannan · G. Viruthagiri · N. Shanmugam · R. Gobi · P. Praveen

Received: 13 October 2013 / Accepted: 3 July 2014 / Published online: 24 July 2014

Abstract TiO_2 nanoparticles doped with different concentrations of cobalt (4, 8, 12 and 16 %) were synthesized by sol–gel method at room temperature with appropriate reactants. In general, TiO_2 can exist in anatase, rutile, and brookite phases. In this present study, we used titanium tetra iso propoxide and 2-propanol as a common starting materials and the obtained products were calcined at 500 °C and 800 °C to get anatase and rutile phases, respectively. The crystalline sizes of the doped and undoped TiO_2 nanoparticles were observed with X-ray diffraction (XRD) analysis. The functional groups of the samples were identified by Fourier transform infrared spectroscopy (FTIR). From UV–VIS diffuse reflectance spectra (DRS), the band gap energy and excitation wavelength of doped and undoped TiO_2 nanoparticles were identified. The defect oriented emissions were seen from photoluminescence (PL) study. The spherical uniform size distribution of particles and elements present in the samples was determined using two different techniques viz., scanning electron microscopy (SEM) with energy-dispersive spectrometer (EDX) and transmission electron microscope (TEM) with selected area electron diffraction (SAED) pattern. The second harmonic generation (SHG) efficiency was also found and the obtained result was compared with potassium di hydrogen phosphate (KDP).

B. Rajamannan (✉)
Department of Engineering Physics, (FEAT), Annamalai University, Annamalainagar, Chidambaram, Tamilnadu 608002, India
e-mail: mugugum@gmail.com

S. Mugundan · G. Viruthagiri · N. Shanmugam · R. Gobi · P. Praveen
Department of Physics, Annamalai University, Annamalainagar, Chidambaram, Tamilnadu 608002, India

Keywords Cobalt · Doped TiO_2 · Nanoparticles · Crystalline size · FTIR · Optical properties

Introduction

Titanium dioxide or titania (TiO_2) was first produced commercially in 1923. It is obtained from a variety of ores. The bulk material of TiO_2 is widely nominated for three main phases of rutile, anatase and brookite. Among them, the TiO_2 exists mostly as rutile and anatase phases which both of them have the tetragonal structures. However, rutile is a high-temperature stable phase and has an optical energy band gap of 3.0 eV (415 nm), anatase is formed at a lower temperature with an optical energy band gap of 3.2 eV (380 nm) and refractive index of 2 (Thamaphat et al. 2008). Among these polymorphs, rutile and anatase have been widely studied. Brookite is rarely studied due to its complicated structure and difficulties in sample preparation (Hu et al. 2009). These three phases can be commonly described as constituted by arrangements of the same building block-Ti–O_6 octahedron in which Ti atom is surrounded by six oxygen atoms situated at the corners of a distorted octahedron. In spite of the similarities in building blocks of Ti–O_6 octahedra for these polymorphs, the electronic structures are significantly different (Guangshe et al. 2011). Photocatalysis using TiO_2 as a catalyst has been widely reported as a promising technology for the removal of various organic and inorganic pollutants from contaminated water and air because of its stability, low cost, and non-toxicity (Liu et al. 2008).

TiO_2 is the promising material as semiconductor having high photochemical stability and low cost. Well-dispersed titania nanoparticles with very fine sizes are promising in

many applications such as pigments, adsorbents, and catalytic supports (Ramakrishna and Ghosh 2003).

Since Fujishima and Honda discovered the photocatalytic splitting of water on a TiO_2 electrode under ultraviolet (UV) light, many synthesis methods for preparing TiO_2 nanoparticles and their applications in the environmental (photo catalysis and sensors) and energy (photovoltaics, water splitting, photo/electrochromics, and hydrogen storage) fields have been investigated (Shan and Demopoulos 2010). Recently, fine particles of titania have attracted a great deal of attention, because of their specific properties as an advanced semiconductor material, such as a solar cell, luminescent material, and photocatalyst for photolysis of water or organic compounds and for bacteriocidal action (Sugimoto et al. 2003).

The Co-doped TiO_2 nanocrystals have consumed great attention due to its enhanced photocatalytic activity (Yang et al. 2007). In this paper, we report the preparation of different weight percentages of Co-doped TiO_2 nanoparticles by a sol–gel route.

Materials and methods

Sample preparation

Preparation of bare and cobalt-doped TiO_2 nanopowder

Sol–gel technique was used to prepare bare and cobalt-doped TiO_2 samples. 90 ml of 2-propanol was taken as a primary precursor and 10 ml titanium tetra isopropoxide was added to it drop wise with vigorous stirring during the process of TiO_2 formation. The solution was vigorously stirred for 45 min to form sols. Liquid solution cobalt nitrate of desired concentration (4, 8, 12, and 16 %) was poured slowly drop by drop to that mixture with continued stirring. To obtain nanoparticles, the obtained gels were dried at 80 °C for 5 h to evaporate water and organic material to the maximum extent. Finally, the powders were kept in muffle furnace and calcinated at 500 °C for 5 h for the harvest of anatase phase and 800 °C for rutile phase. The particle was pulverized to powder using an agate mortar at room temperature for further characterizations.

Sample characterization

The bare and Co-doped TiO_2 anatase are subjected into different characterizations, such as powder XRD, FTIR, UV-DRS, PL, SEM with EDX, TEM with SAED pattern, and SHG (NLO). The crystalline phase and particle size of TiO_2 nanoparticles were analyzed by X-ray diffraction (XRD) measurement, which was carried out at room temperature using XPERT-PRO diffractometer system (scan step of 0.05°, counting time of 10.16 s per data point) equipped with a Cu tube for generating Cu $K\alpha$ radiation ($\lambda = 1.5406$ Å). The incident beam in the 2-theta mode over the range of 20°–80°, operated at 40 kV and 30 mA. The chemical structure was investigated by AVATAR 330 Fourier transform infrared spectrometer (FTIR) in which the IR spectrum was recorded by diluting the mixed powder in KBr and in the wavelength between 4,000 and 400 cm^{-1}. The band gap energy and the particle size were measured at wavelength in the range of 200−2,500 nm by UV–VIS–NIR spectrophotometer (varian/carry 5000) equipped with an integrating sphere and the baseline correction was performed using a calibrated reference sample of powdered barium sulfate ($BaSO_4$). The photoluminescence spectra (PL) are recorded with Perkin Elmer LS fluorescence spectrophotometer. Scanning electron microscope (SEM) images were observed with a Hitachi S-4800 microscope, combined with energy-dispersive X-ray spectroscopy (EDX, Oxford 7021) for the determination of elemental composition. Transmission electron microscope (TEM) with selected area electron diffraction (SAED) images were taken using a technai t20 operated at a voltage of 200 kV. The NLO property of the materials was confirmed by the Kurtz powder second harmonic generation (SHG) test. A Q-switched Nd-YAG laser whose output was filtered through 1,064 nm narrow pass filter was used for this purpose. The input power of the laser beam was measured to be 4.5 m J/pulse.

Results and discussion

Powder X-ray diffraction study (XRD)

Figure 1 exhibits the XRD patterns of bare and cobalt-doped TiO_2 nanocrystals calcined at 500 °C for 5 h. From

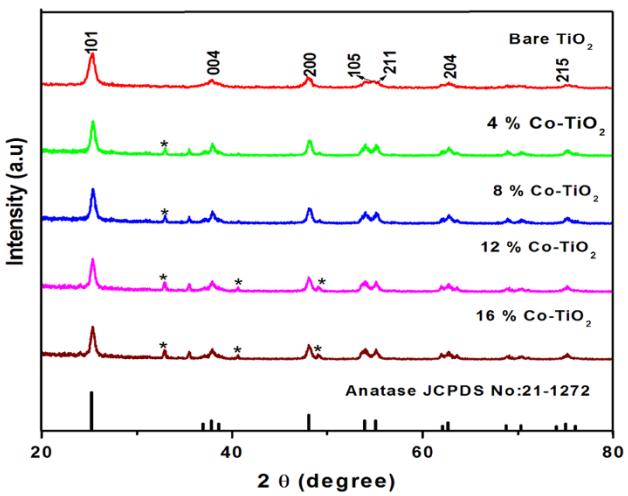

Fig. 1 X-ray diffraction pattern for bare TiO_2 and Co-doped TiO_2 nanoparticle

Table 1 Crystallite sizes for the bare and Co-doped TiO_2 nanoparticle

Samples	Crystallite size (nm)
Bare TiO_2	15.31
4 % Co-doped TiO_2	19.9092
8 % Co-doped TiO_2	20.9140
12 % Co-doped TiO_2	23.4380
16 % Co-doped TiO_2	25.9223

the diffraction patterns, it is noted that bare and cobalt-doped TiO_2 are in anatase phase rather than rutile or brookite (JCPDS Card no 21-1272). The XRD patterns obtained in the present study are identical with the earlier report (Karthik et al. 2010). At low level of cobalt incorporation, the XRD patterns do not show any cobalt phase, indicating that cobalt ions are uniformly dispersed on the host TiO_2. However, at high level of Co^{2+} incorporation (12 and 16 wt%), peaks related to cobalt are started to appear which are marked by a symbol star.

From the obtained peaks, the average nanocrystallite size was measured according to using Debye–Scherrer formula, the Eq. (1).

$$D = \frac{K\lambda}{\beta \mathrm{Cos}\theta} \quad (1)$$

where D is the crystallite size, K is the shape factor, $\lambda = 0.154$ nm, β is the full width at half maximum, θ is the reflection angle and the results are presented in Table 1. In comparison with undoped TiO_2, all the doped products show increased particle size. The increased particle size may be explained by the fact that the ionic radius of Co^{2+} (0.74 Å) is greater than that of Ti^{4+} (0.60 Å) (Liu et al. 2008).

Fourier transform infrared spectroscopy (FTIR)

Figure 2 shows the FTIR spectra of the obtained bare and Co-doped TiO_2 nanoparticles after calcined at 500 °C for 5 h. The peak positioned at 3,415 cm^{-1} is attributed to O–H stretching vibration. The peaks appearing at 1,629 cm^{-1} were attributed to H–O–H bending vibration mode of physically observed water. Appearance of Ti–O–Ti frequency absorption is noted between 600 and 400 cm^{-1} (Choudhury and Choudhury 2012). The appearance of band at 2,860 cm^{-1} was due to the C–H bond of the organic compounds (Maensiri et al. 2006). The weak band at 2,833 cm^{-1} could be ascribed to the characteristic frequencies of residual organic species, which was not completely removed by ethanol and distilled water washing (Guo et al. 2007; Wang et al. 2007). The two prominent absorption bands at 3,400 and 1,633 cm^{-1} in the materials can be recognized as the stretching and bending vibrations

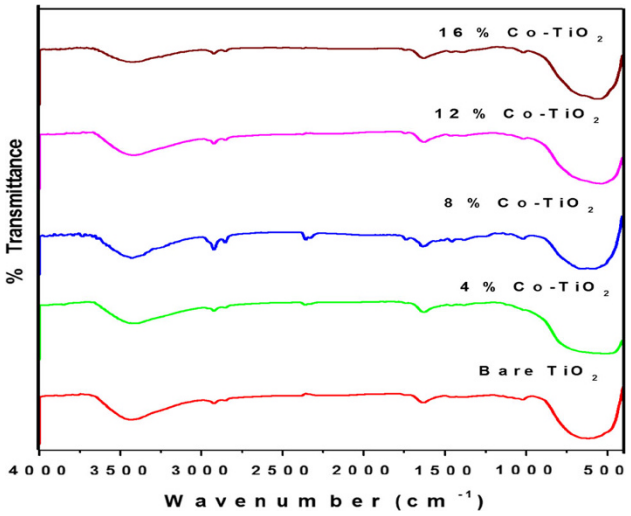

Fig. 2 FTIR spectra pattern for bare TiO_2 and Co-doped TiO_2 nanoparticle

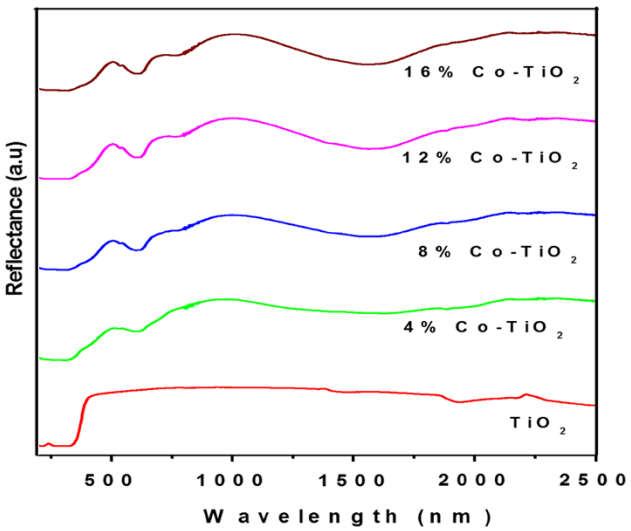

Fig. 3 UV-DRS spectra for bare TiO_2 and Co-doped TiO_2 nanoparticle-direct transition

of water molecules. The intensity of these two bands in Co is diminished compared with bare TiO_2. The peaks in between 2,924 and 2,843 cm^{-1} are assigned to C–H stretching vibrations of alkane groups. The alkane and carboxylic groups specified by different bands are arise from titanium tetra isopropoxide and 2-propanol (precursor material), when we used in the synthesis process. In addition, a broad absorption band between 500 and 1,000 cm^{-1} is ascribed to the vibration absorption of the Ti–O–Ti linkages in TiO_2 nanoparticles (Lu et al. 2008).

Ultra violet-diffuse reflectance spectra (UV-DRS)

The optical properties of samples were characterized by UV-DRS. The diffused reflectance spectra of undoped and

different weight percentages (4, 8, 12 and 16 %) of Co-doped TiO_2 are shown in (Fig. 3).

In anatase phase of TiO_2, Ti^{4+} is surrounded by six oxygen atoms in an octahedral coordination, forming TiO_6 octahedra. When Co^{2+} substitutes Ti^{4+}, it forms bond with six oxygen atoms. Now, according to crystal field theory, the electrons in the d-orbital of Co^{2+} will undergo repulsion by the electrons of the six surrounding oxygen atoms. This results in the splitting of d-orbital of Co^{2+}, showing the aforementioned d–d transition. These types of electronic transition will be by Co^{2+} when it substitutes Ti^{4+} and remains in octahedral or pseudo octahedral coordination (Choudhury and Choudhury 2012). The DRS spectrum of TiO_2 showed a broad intense absorption at around 345 nm due to the charge transfer from the valence band formed by 2p orbitals of the oxide anions to the conduction band formed by 3d t_{2g} orbitals of the Ti^{4+} cations (Sadanandam et al. 2013; Kirit and Dimple 2012).

From the UV–VIS DRS spectra (Fig. 3), bare TiO_2 particles exhibit strong absorption at $\lambda < 400$ nm. Compared to the spectrum of bare TiO_2, there is a new absorption band present between 400 and 800 nm of all samples, which means band gap absorption onset was extended into the visible light region for all Co-doped TiO_2 samples. The absorption bands at 200−400 nm are due to the charge transfer from the valence band to the conduction band of TiO_2.

However, on 12 % Co^{2+} doping, the absorption spectrum is positioned at 748 nm. At 16 % of doping, the absorption peak is blue shifted to 742 nm. On increasing the concentration of doping, the value of blue shift increases with the enhancement in the intensity of visible band. The band gap energies were calculated from the cut-off wavelength of bare and Co-doped TiO_2 using the Eq. (2).

$$E_g = \frac{hc}{\lambda}\text{eV};\ E_g = \frac{1,240}{\lambda}\text{eV} \quad (2)$$

where E_g is the band gap energy (eV), h is the Planck's constant (6.626×10^{-34} Js), c is the light velocity (3×108 m/s), and λ is the wavelength (nm).

The calculated values are 3.58 eV (345 nm), 3.65 eV (339 nm), 3.75 eV (330 nm), 3.81 eV (325 nm), and 3.93 eV (315 nm) for bare TiO_2 and TiO_2 doped with 4, 8, 12, and 16 wt% of Co^{2+}, respectively, and are given in (Table 2).

Table 2 Band gap energy for bare and Co-doped TiO_2 nanoparticle

Samples	Band gap (eV)
Bare TiO_2	3.58
4 % Co-doped TiO_2	3.65
8 % Co-doped TiO_2	3.75
12 % Co-doped TiO_2	3.81
16 % Co-doped TiO_2	3.93

From the Table 2, it is noted that bare TiO_2 nanoparticle has a larger band gap (3.58 eV) than that of bulk TiO_2 nanomaterial (3.2 eV), which is quite expected due to quantum confinement effect. But, after various levels of cobalt doping, the band gap is running between 3.65 and 3.93 eV.

Photoluminescence (PL)

PL emission spectra of bare and 16 wt% of Co-doped TiO_2 with 300 nm excitation are shown in (Fig. 4). The PL spectrum of TiO_2 exhibits a UV emission (373 nm) and two visible emissions: one at 431 nm and the other at 587 nm. The UV emission is considered as the band edge emission of the host TiO_2, and the 431 nm peak can be ascribed to self-trapped excitations localized in TiO_6 octahedra (Wan et al. 2010). The existences of green emission peak at 587 nm explain the presence of oxygen vacancies (Abazovic et al. 2006). When compared with bare TiO_2, the PL emission bands of doped product are blue shifted with intensity reduction in the UV band and enhancement in the visible bands (Kirit and Dimple 2012).

Scanning electron microscope (SEM with EDX)

Figures 5 and 6 show typical scanning electron microscopic images of bare and 16 wt% Co-doped TiO_2 nanoparticle. From the figures, the most of the particles are almost spherical in shape with uniform size distribution (Reddy et al. 2010). It is evident that the growth of particle is restrained by Co on doping with TiO_2. A closer examination of these figures reveals a well-defined particle like morphology, having abundance of spherical-shaped particles, with the average agglomerated particle size in the range of 15.31−25.92 nm. The spherical shape is

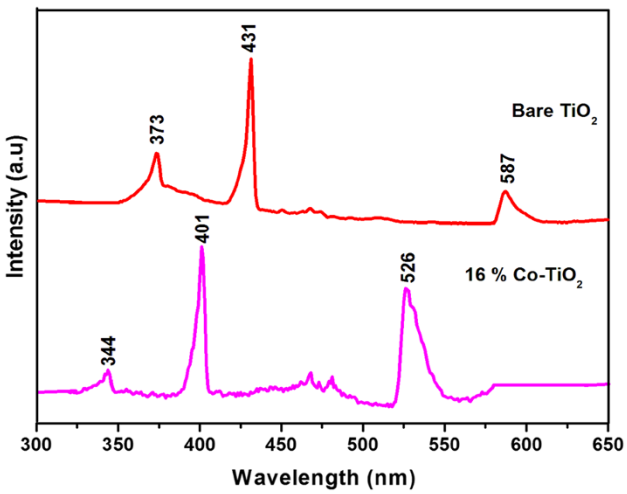

Fig. 4 PL spectra for bare TiO_2 and Co-doped TiO_2 nanoparticle

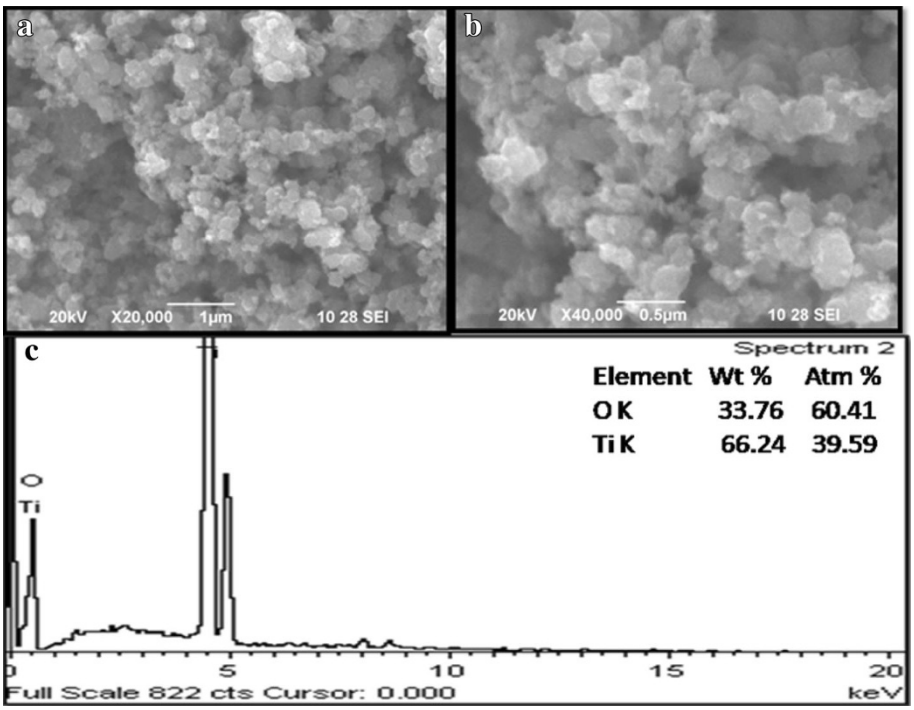

Fig. 5 SEM micrograph of TiO_2 nanoparticles (**a**, **b**) and corresponding to EDX diagram (**c**)

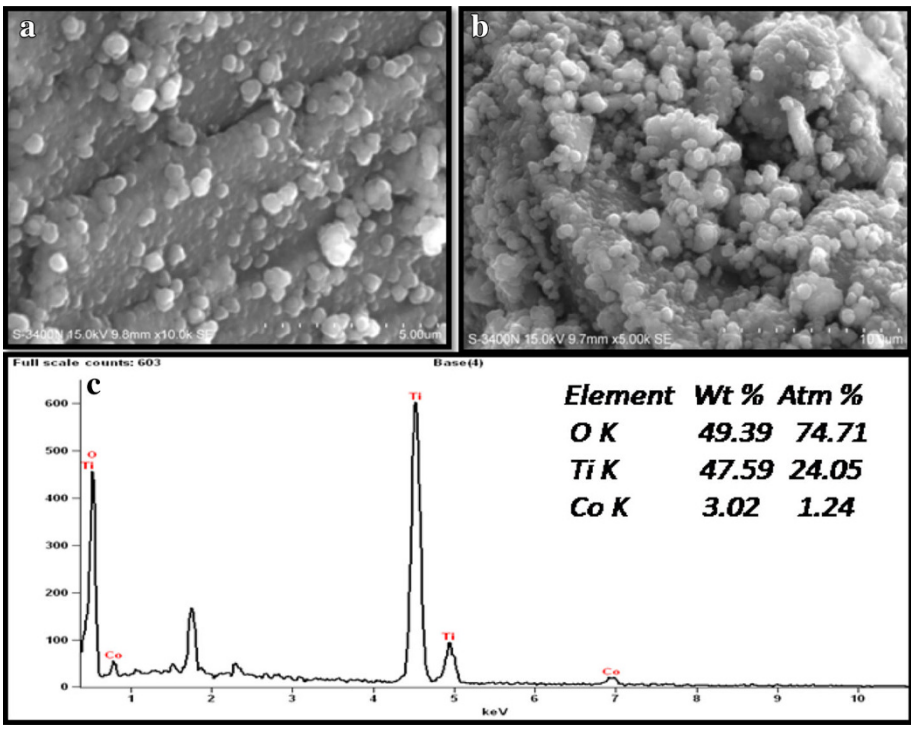

Fig. 6 SEM micrograph of Co-doped TiO_2 nanoparticles (**a**, **b**) and corresponding to EDX diagram (**c**)

significantly important not only for the design of surface properties and surface area, but also for tuning the electronic structure i.e., to make the visible light spectrum more active for the better photocatalytic activity (Narayana et al. 2011).

Energy-dispersive X-ray spectroscopy (EDAX) of 16 wt% of Co-doped TiO_2 (Figs. 5c, 6c) shows the presence of O, Ti and cobalt according to atomic weight stoichiometric of 74.71, 24.05 and 1.24 %, respectively (Kirit and Dimple 2012).

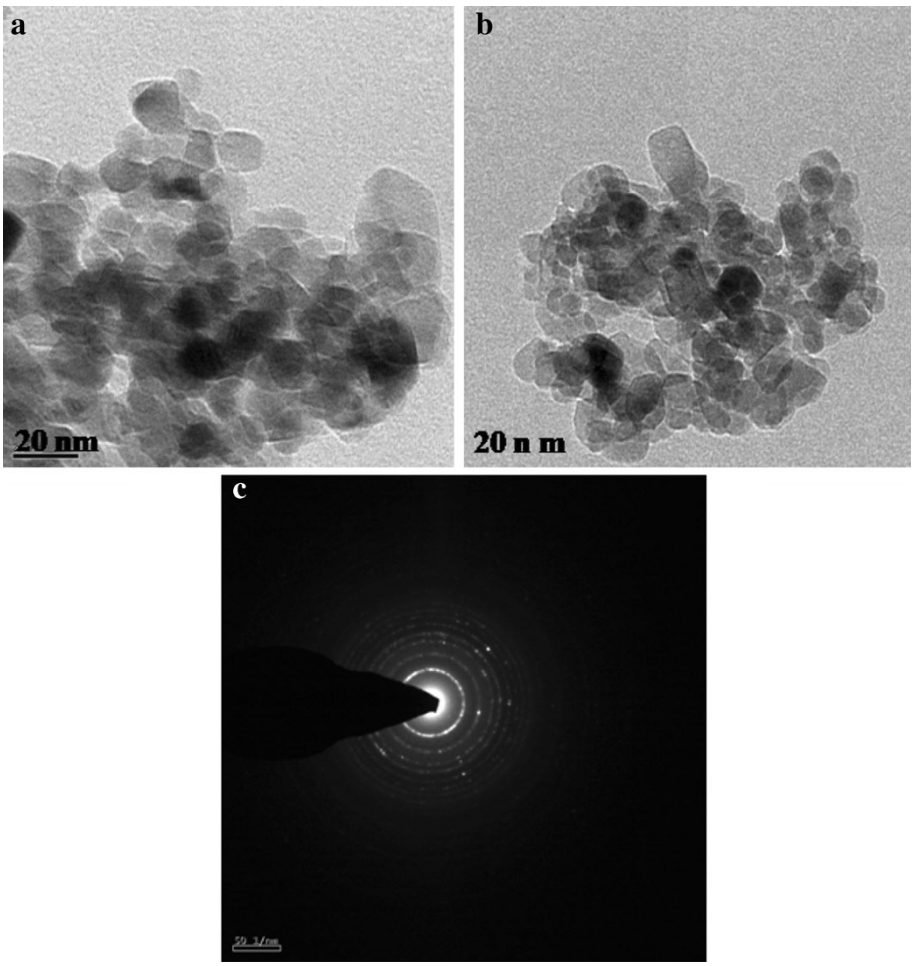

Fig. 7 TEM image of bare TiO_2 nanoparticles (**a**, **b**) and corresponding to SAED pattern (**c**)

Transmission electron microscope (TEM)

Figures 7a, b and 8a, b illustrate the transmission electron microscope (TEM) images of the bare and 16 wt% Co-doped TiO_2 nanoparticles obtained after 500 °C of annealing. They showed almost spherical shape particles with uniform size distribution. As can be seen from the TEM image that the particle sizes are in the range of 15–25 nm, which is in good agreement with the crystallite size obtained from XRD results. In general, TiO_2 nanoparticles appear in transparent spherical shape. On incorporation of cobalt particles dark patches are seen on the surface of transparent TiO_2 nanoparticles. Electron diffraction patterns showed the brightness and intensity of polymorphic discrete ring of the highly crystalline nanoparticles are shown in (Figs. 7c and 8c).

Non-linear optical studies

For the preparation of NLO study, the oven-dried powders of bare TiO_2 and 16 wt% Co-doped TiO_2 were kept into muffle furnace and annealed at 800 °C for 5 h to obtain the rutile phase. The study of non-linear optical conversion efficiency was carried out using the experiment setup of Kurtz and Perry. A Q-switched Nd-YAG laser beam of wavelength 1,064 nm, with a repetition rate of 10 Hz was used. The bare TiO_2 and Co-doped TiO_2 were nano-powdered with a uniform particle size and then packed in a microcapillary of uniform bore and exposed to laser radiations. The SHG was confirmed by the emission of green radiation of 532 nm wavelengths and the parent ray was filtered using IR filter. A sample of potassium di hydrogen phosphate (KDP) also powdered to the same particle size as the experimental sample was used as a reference material in the present measurement. The relative SHG measurement gave conversion efficiency of bare TiO_2. Thus, the efficiency shows an output of 8.0 mV for bare TiO_2, 6.0 mV for Co-doped TiO_2 and 10.2 mV for KDP. When compared to 10.2 mV of KDP, for same input laser power, the bare and Co-doped TiO_2 show lesser second harmonic efficiencies. The calculated results are represented in Table 3.

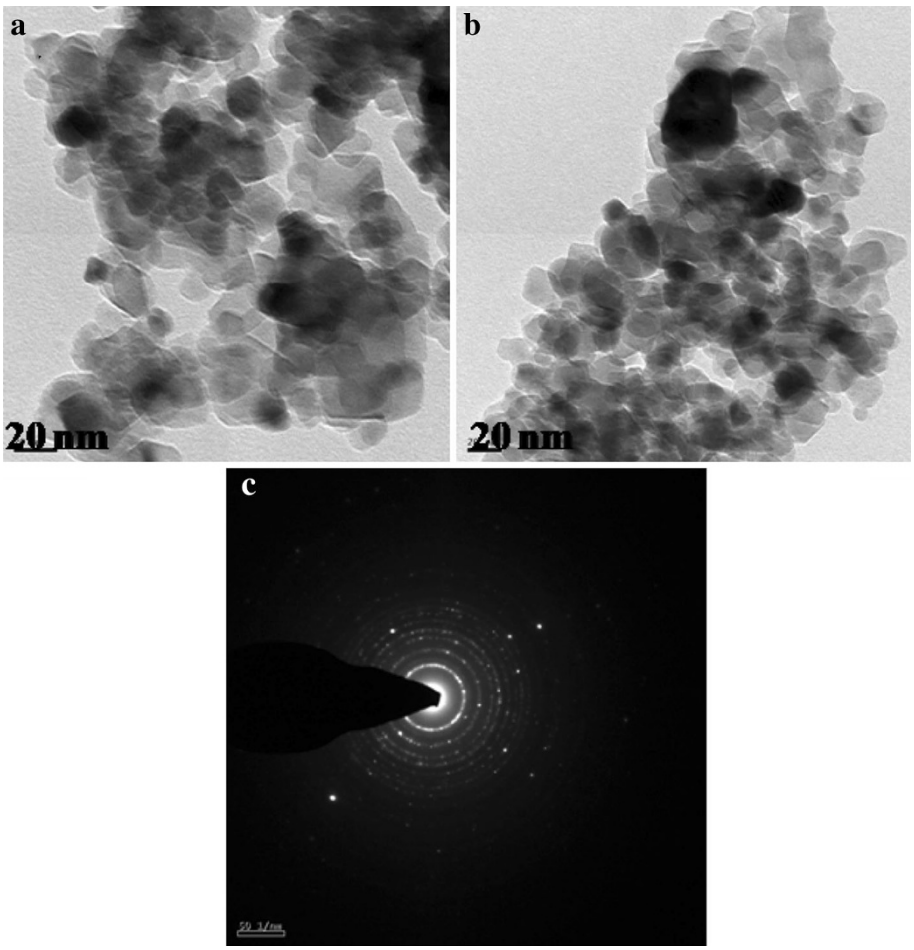

Fig. 8 TEM image of Co-doped TiO_2 nanoparticles (**a**, **b**) and corresponding to SAED pattern (**c**)

Table 3 Comparision of SHG efficiency of bare and 16 % Co-doped TiO_2 nanoparticles

Samples	Input (mJ/pulse)	Output (mV)	KDP (mV)	SHG efficiency
Bare TiO_2	4.5	8.0	10.2	0.78
Co-doped TiO_2	4.5	6.0	10.2	0.58

Conclusion

We have successfully synthesized the bare and different weight percentages (4, 8, 12 and 16 %) of Co-doped TiO_2 nanoparticles by means of sol–gel method at room temperature. The synthesized products were annealed at 500 and 800 °C for getting anatase and rutile phases, respectively. The annealed samples were characterized by the techniques like XRD, FTIR, and UV-DRS. The doping concentration of 16 wt% was chosen for further analysis like PL, SEM with EDX, TEM with SAED pattern, and NLO. From the results of XRD patterns, it is confirmed that the TiO_2 was in anatase phase with crystallite sizes in the range of 15.31−25.92 nm. In comparison with undoped TiO_2, all the doped products show increased particle size. The existences of functional groups were identified by FTIR analysis. The cut-off wavelengths were identified by UV–VIS DRS analysis and the band gap energies of the undoped and doped products are having values between 3.58 and 3.93 eV. The PL emission spectra show the creation of new luminescent centers. The SEM with EDX and TEM image with SAED pattern confirm the spherical morphology of the products. In SHG, bare TiO_2 shows greater NLO efficiency than the doped product.

References

Abazovic ND, Mirjana IC, Miroslav DD, Jovanovic DJ, Phillip AS, Jovan MN (2006) Photo luminescence of anatase and rutile TiO_2 particles. J Phys Chem B 110:25366–25370

Choudhury B, Choudhury A (2012) Luminescence characteristics of cobalt doped TiO_2 nanoparticles. J Lumin 132:178–184

Guangshe L, Liping L, Jing Z (2011) Understanding the defect chemistry of oxide nanoparticles for creating new functionalities. Inorg Solid State Chem Energy Mater 54:876–886

Guo GS, He CN, Wang ZH, Gu FB, Han DM (2007) Synthesis of titania and titanate nanomaterials and their application in environmental analytical chemistry. Talanta 72:1687–1692

Hu WB, Li LP, Li GS, Tang CL, Sun L (2009) High-quality brookite TiO_2 flowers: synthesis, characterization, and dielectric performance. Cryst Growth Des 9:3676–3682

Karthik K, Pandian SK, Kumar KS, Jaya NV (2010) Influence of dopant level on structural, optical and magnetic properties of Co-doped anatase TiO_2 nanoparticles. Appl Surf Sci 256:4757–4760

Kirit S, Dimple S (2012) Characterization of nanocrystalline cobalt doped TiO_2 sol–gel material. J Cryst Growth 352:224–228

Liu XH, He XB, Fu YB (2008) Effects of doping cobalt on the structures and performances of TiO_2 photocatalyst. Acta Chim Sinica 66:1725–1730

Lu X, Xiuqian L, Zhijie S, Zheng Y (2008) Nanocomposite of poly (L-lactide) and surface-grafted TiO_2 nanoparticles: synthesis and characterization. Eur Polym J 44:2476–2481

Maensiri S, Laokul P, Klinkaewnarong J (2006) A simple synthesis and room-temperature magnetic behavior of Co doped anatase TiO_2 nanoparticle. J Magn Magn Mater 302:448–453

Narayana RL, Matheswaran M, Aziz AA, Saravanan P (2011) Photocatalytic decolourization of basic green dye by pure and Fe, Co doped TiO_2 under daylight illumination. Desalination 269:249–253

Ramakrishna G, Ghosh HN (2003) Optical and photochemical properties of sodium dodecylbenzene sulfonate (DBS) capped TiO_2 nanoparticles dispersed in nonaqueous solvents. Langmuir 19:505–508

Reddy MV, Jose R, Teng TH, Chowdari BVR, Ramakrishna S (2010) Preparation and electrochemical studies of electrospun TiO_2 nanofibers and molten salt method nanoparticles. Electrochim Acta 55:3109–3117

Sadanandam G, Lalitha K, Kumari VD, Shankar MV, Subrahmanyam M (2013) Cobalt doped TiO_2: a stable and efficient photocatalyst for continuous hydrogen production from glycerol: water mixtures under solar light irradiation. Int J Hydrogen Energy 38:9655–9664

Shan GB, Demopoulos GP (2010) The synthesis of aqueous-dispersible anatase TiO_2 nanoplatelets. Nanotechnology 21:1–9

Sugimoto T, Zhou X, Muramatsu A (2003) Synthesis of uniform anatase TiO_2 nanoparticles by gel–sol method formation process and size control. J Colloid Interface Sci 259:43–52

Thamaphat K, Limsuwan P, Ngotawornchai B (2008) Phase characterization of TiO_2 powder by XRD and TEM. Nat Sci 42:357–361

Wan WY, Chang YM, Ting JM (2010) Room-temperature synthesis of single-crystalline anatase TiO_2 nanowires. Cryst Growth Des 10:1646–1651

Wang X, Song X, Lin M, Wang H, Hao Y, Zhong W, Du Q (2007) Surface initiated graft polymerization from carbon-doped TiO_2 nanoparticles under sunlight illumination. Polymer 48:5834–5838

Yang X, Cao C, Hohn K, Erickson L, Maghrang R, Hamal D, Klabunde K (2007) Highly visible-light active C- and V-doped TiO_2 for degradation of acetaldehyde. J Catal 252:296–302